In addition to this, the nanosize diameter of CNT fibres, a few to several tens of nm, is close to that of filopodia of cells, approximately 100 nm as seen in figure 18*b*, which provides easy conditions for the filopodia to interact with a CNT network. Trypsin is generally used for the detachment of cells from a scaffold. On a CNT scaffold, however, cells cannot separate well because of the strong binding of filopodia, which is sometimes mechanical binding, with a CNT network. It demonstrates the good cell adhesivity of CNTs (Aoki *et al.* 2005). Bacteria of submicron to micrometre size are also trapped by the fine, wavy nanodiameter of a SWCNT string in the manner of winding around them (Akasaka & Watari 2009). These are another example that micro/nano-sized materials become biointeractable with biological objects of comparable size, in these cases with filopodia and bacteria. The Nano-meshwork structure of CNT agglomeration contributes physically to favoured conditions for cell attachment.

4.14. Invasion and internal diffusion of nanoparticles

Stimulus, represented by an amount of TNF-α release in figure 11, which is pronounced below 10 μm, exhibited the maximum from around μm down to 500 nm. For smaller sizes below 200 nm, more typically less than 50 nm, stimulus decreased to nearly the level of macroscopic size (Watari *et al.* 2007*a*). This looks preferable from the point of view of biological application of nanoparticles, since toxicity is apparently decreased. However, this, in turn, means that the biophylactic system does not work well any more against nanoparticles. The invasion of nanoparticles into the body can occur for this range of particle size. Nanoparticles might be the objects whose existence has not been assumed in the body defence system of a living organism.

It is known that particles below 10 μm can pass through the bronchial. For further smaller ones, they may reach lung pulmonary alveoli where they are taken up directly into blood vessels. Thus, they can invade into the internal body through the respiratory system (figure 12) and also through the digestive system at the intestinal wall (figure 13). Then they diffuse through the cardiovascular system for the whole body from organ to organ (figure 14). The behaviour of internal diffusion is different, depending on materials, for example, TiO_2 and Pt (Watari *et al.* 2007*c*,*d*, 2008*a*, 2009; Abe *et al.* 2009, in press *a*,*b*,*c*).

4.15. Non-specificity of particle-inducing bioreaction

There are many pathways for living organisms to recognize foreign objects. Macrophages discriminate biohazardous objects such as bacteria and make an initial response specific to each object. The absolute intensity of TNF-α expression against endotoxin or lipopeptide is far higher than physical size effect. Toxicity by bacteria or rejection response caused by certain proteins is much stronger. One of the recognition paths is through the toll-like receptor (TLR). In some cases, they discriminate by different sugar chain patterns. In this way, both innate and acquired immune systems work against micro-organisms and proteins, mostly in specific manner.

On the other hand, in the case of materials, the present *in vitro* and *in vivo* experiments showed that (i) a similar particle size dependence of expression of superoxide and cytokines irrespective of the different nature of materials with bioinert or bioactive properties (figure 9).

These indicate that (ii) the reaction is non-specific and any particles below cell size are regarded as foreign objects by cells including neutrophils and macrophages, which induces phagocytosis whatever the material as observed *in vitro* (figure 3) and *in vivo* (figures 4 and 10).

(iii) Toxicity level shown as an absolute intensity of superoxide production, cytokines IL-1β and TNF-α expression by micro/nanoparticles is very low compared with endotoxin (Kiura *et al.* 2005; Watari *et al.* 2007*a*).

(iv) TLR is not sensitive and rather inert to particles of materials according to our different studies.

There is always a serious rejection reaction for organ transplantation from one person to another, where the difference in individuals is discriminated in a specific identification manner. (v) For the case of materials such as in an implant, there is no strong rejection and it is commonly and generally, therefore, acceptable to any person.

All these demonstrate that the acquired immune systems do not work and only some of the innate immune systems are activated against materials. Non-actuation of immune systems, except a few innate immunity processes and lack of other recognition paths to materials, limits the recognition routes and reactions to fewer possibilities. One of the most frequently encountered actuations is a phagocytosis reaction with the dependency only on particle size, and another is stimulus, sometimes mechanical, by particle shape when a pointing needle form. This lack of recognition paths shows the characteristics of an non-specific nature to particle bioreaction, occurring irrespective of materials. The lack of recognition paths is also one of the central reasons that the body defence system cannot respond well to nanoparticles, and (vi) they can invade directly into the internal body through the respiratory and digestive system, rather easily and non-specifically.

These numbered facts (i)–(vi) in the above symbolize the non-specificity in the characteristics of nanoparticles in relation to biological organisms.

4.16. Biointeractable critical size: relationships with cells and viruses

The critical sizes where the transition of material behaviour against biological organisms occurs are at approximately 100 μm, 10 μm and 200 nm. Materials start to behave with the characteristics of particles from approximately 100 μm and below. In the case of a needle shape, this critical value would be larger to some extent. The critical sizes, 10 μm to become biointeractable

through the induction of phagocytosis in cells and inflammation to tissues and 200 nm, most typically less than 50 nm, to be less stimulative and become able to invade into the body, are approximately coincident with the average size of cells and viruses, respectively.

Is there any reason for these critical sizes to be the level of cell and virus? This coincidence may not be by accident.

When the particle size becomes nearly the same as cell size, approximately 10 μm or smaller, the object becomes biointeractive. Macrophages discriminate objects and initiate specific reactions, which are followed by the activation of T lymphocytes and others against bacteria and virus. In the case of materials, most such immune systems and recognition paths do not work and only the process that senses the particle size remains, regarding non-specifically the objects smaller than cells as foreign objects. This induces phagocytosis, followed by the formation of lysosome in cells and treatment in it.

The lack of recognition paths in the immune system makes objects of a size similar to viruses less stimulative. The insufficient immunity makes them able to invade the internal body and cells through the pulmonary alveolus, intestine or other paths as viruses can enter. This is in contrast to the case of a virus where the specific immune system is actuated and invasion may be blocked. Thus, the object size permissible to invade becomes the level of virus.

4.17. Antagonism of nanotechnology and nanotoxicology

The recognition of physical particle size and shape effect is the essential basis for the proper understanding of the nanosizing effect and for the development of biomedical applications of nanotechnology. High function and risk assessment often produces antagonism of nanotechnology and nanotoxicology between nanotech-developing researchers and toxicologists. From the viewpoint of bioreactivity of the nanosizing effect as revealed in the present study, they are different sides of an evaluation system for human beings, merit if they match the purpose of human beings or demerit if they unintentionally appear against. However, both originate from the same mechanism. It is necessary to recognize the bilateral nature of nanomaterials, high function and risk, for the proper acknowledgement of the influence on biological organisms and environments and for the development and application of nanotechnology.

5. CONCLUSIONS

The increase in specific surface area usually counted as the nanosizing effect causes the enhancement of chemical reactivity and serious toxicity for soluble and stimulative materials. This is the contribution of compositional effects, and is easily recognized. This effect originates solely from material properties and greatly enhances the same functions as those of a macroscopic size. Catalysts are a typical example of this effect and no biological interaction is involved.

Non-soluble, biocompatible materials show different particle size dependence. The transition of bioreaction occurs at the critical sizes of approximately 100 μm, 10 μm and 200 nm. This physical size effect is non-specific, which is independent of material type, and especially pronounced for a cell size of less than approximately 10 μm. It causes stimulus through the biological process of phagocytosis in cell and inflammation in tissue. When the particle size is 200 nm or less, they become less stimulative and the recognition by body defence systems becomes weaker. They may invade directly into the internal body through the respiratory or digestive system and diffuse inside the whole body.

Thus, the physical micro/nanosizing of materials makes them biointeractive with cells and tissue. These biointeractable particles induce the intrinsic functions and reactions of biological organisms. They become bioreactive and may work both in merit and demerit ways. The bioreactive nature causes inflammation, and this leads to the occurrence of conversion of functions of materials through biological processes such as from biocompatibility to stimulus in Ti-abraded particles and asbestos, from non-bone substitutional to bone substitutional in nanoapatite and from non-cell adhesive to cell adhesive CNTs.

This effect has its origin in the biological interaction process between particles and cells/tissue. Non-actuation of immune system, except for a few innate immunity processes and limitation of recognition paths for materials, gives the non-specific nature to particle bioreaction and restricts the recognition routes to the size-sensitive phagocytosis reaction. This insensitive nature also permits nanoparticles below 200 nm to slip through the body's defence system and invade directly into the internal body.

The characteristic phenomena of no rejection reactions to artificial organs in macro, non-specific phagocytosis to cells and inflammation to tissue in micro and direct invasion into the internal body in nano originate on the same basis that the actuation of immune system is limited to the few possibilities of innate immunity for materials.

The acknowledgement of the physical particle size effect and the bilateral nature of nanomaterials with possibilities of high functions and risks is the essential basis for the proper understanding of the nanosizing effect and for the development of biomedical applications of nanotechnology.

Animal experiments were performed in accordance with the Guide for the Care and Use of Laboratory Animals, Hokkaido University Graduate School of Dental Medicine.

The present study was performed under the support of Health and Labour Sciences Research Grants in Research on Chemical Substance Assessment from the Ministry of Health, Labour and Welfare of Japan (H18-Chemistry-General-006).

REFERENCES

Abe, S., Koyama, C., Akasaka, T., Uo, M., Kuboki, K. & Watari, F. 2009 Internal distribution of several inorganic microparticles in mice. *Bioceramics* **21**, 539–542. (Key engineering materials, vols. 396–398; *Trans. Tech. Publications*)

Abe, S. *et al.* In press *a*. Biodistribution imaging of magnetic nanoparticles in mice compared with X-ray scanning analytical microscopy and magnetic resonance imaging. *Bio-Med. Mater. Eng.*

Abe, S., Koyama, C., Esaki, M., Akasaka, T., Uo, M., Kuboki, K., Morita, M. & Watari, F. In press *b*. *In vivo* internal diffusion of several inorganic microparticles through an oral administration. *Bio-Med. Mater. Eng.*

Abe, S., Koyama, C., Uo, M., Akasaka, T., Kuboki, K. & Watari, F. In press *c*. Time-dependence and visualization of TiO_2 and Pt particle biodistribution in mice. *J. Nanosci. Nanotechnol.*

Akasaka, T. & Watari, F. 2005 Nano-architechture on carbon nanotube surface by biomimetic coating. *Chem. Lett.* **34**, 826–827. (doi:10.1246/cl.2005.826)

Akasaka, T. & Watari, F. 2008 Carbohydrate coating of carbon nanotubes for biological recognition. *Fullerenes Nanotubes Carbon Nanostruct.* **16**, 114–125. (doi:10.1080/15363830801887992)

Akasaka, T. & Watari, F. 2009 Capture of bacteria by flexible carbon nanotubes. *Acta Biomater.* **5**, 607–612. (doi:10.1016/j.actbio.2008.08.014)

Akasaka, T., Watari, F., Sato, Y. & Tohji, K. 2005 Apatite formation on carbon nanotubes. *Mater. Sci. Eng. C* **26**, 675–678. (doi:10.1016/j.msec.2005.03.009)

Akasaka, T., Yokoyama, A., Matsuoka, M., Hashimoto, T., Abe, S., Uo, M. & Watari, W. In press *a*. Adhesion of human osteoblast-like cells (Saos-2) to carbon nanotube sheets. *Bio-Med. Mater. Eng.*

Akasaka, T., Nakata, K., Uo, M. & Watari, F. In press *b*. Modification of the dentin surface by using carbon nanotubes. *Bio-Med. Mater. Eng.*

Aoki, N., Yokoyama, A., Nodasaka, Y., Akasaka, T., Uo, M., Sato, Y., Tohji, K. & Watari, F. 2005 Cell culture on a carbon nanotube scaffold. *J. Biomed. Nanotechnol.* **1**, 402–405. (doi:10.1166/jbn.2005.048)

Aoki, N., Yokoyama, A., Nodasaka, Y., Akasaka, T., Uo, M., Sato, Y., Tohji, K. & Watari, F. 2006 Strikingly extended morphology of cells grown on carbon nanotubes. *Chem. Lett.* **35**, 508–509. (doi:10.1246/cl.2006.508)

Aoki, N., Akasaka, T., Watari, F. & Yokoyama, A. 2007*a* Carbon nanotubes as scaffolds for cell and effect on cellular functions. *Dent. Mater. J.* **26**, 178–185. (doi:10.4012/dmj.26.178)

Aoki, N., Yokoyama, A., Nodasaka, Y., Akasaka, T., Uo, M., Sato, Y., Tohji, K. & Watari, F. 2007*b* Carbon nanotubes deposited on titanium implant for osteoblast attachment. *J. Bionanosci.* **1**, 14–16. (doi:10.1166/jbns.2007.003)

Asakura, K., Chun, W. J., Tohji, K., Sato, Y. & Watari, F. 2005 X-ray absorption fine structure studies on the local structures of Ni impurities in a carbon nanotube. *Chem. Lett.* **34**, 382–383. (doi:10.1246/cl.2005.382)

Chan, W. C. W., Maxwell, D. J., Gao, X., Bailey, R. E., Han, M. & Nie, S. 2002 Luminescent quantum dots for multiplexed biological detection and imaging. *Curr. Opin. Biotechnol.* **13**, 40–46. (doi:10.1016/S0958-1669(02)00282-3)

Fugetsu, B. *et al.* 2004*a* Caged multi-walled carbon nanotubes as the adsorbents for affinity-based elimination of ionic dyes. *Environ. Sci. Technol.* **38**, 6890–6896. (doi:10.1021/es049554i)

Fugetsu, B., Satoh, S., Iles, A., Tanaka, K., Nishi, N. & Watari, F. 2004*b* Encapsulation of multi-walled carbon nanotubes (MWCNTs) in Ba^{2+}-alginate toform coated micro-beads and their application to the pre-concentration/elimination of dibenzo-p-dioxin, dibenzofuran, and biphenyl from contaminated water. *Analyst (London)* **129**, 565–566. (doi:10.1039/b405325g)

Gelinsky, M. *et al.* 2007 Biomaterials based on mineralised collagen an artificial extracellular bone matrix. In *Interface oral health science 2007* (eds M. Watanabe & O. Okuno), pp. 323–328. Tokyo, Japan: Springer.

Kiura, K., Sato, Y., Yasuda, M., Fugetsu, B., Watari, F., Tohji, K. & Shibata, K. 2005 Activation of human monocytes and mouse splenocytes by single-walled carbon nanotubes. *J. Biomed. Nanotechnol.* **1**, 359–364. (doi:10.1166/jbn.2005.031)

Kumazawa, R., Watari, F., Takashi, N., Tanimura, Y., Uo, M. & Totsuka, Y. 2002 Effects of Ti ions and particles on cellular function and morphology of neutrophils. *Biomaterials* **23**, 3757–3764. (doi:10.1016/S0142-9612(02)00115-1)

Li, X. M., Van Blitterswijk, C. A., Feng, Q. L., Cui, F. Z. & Watari, F. 2008*a* The effect of calcium phosphate microstructure on bone-related cells *in vitro*. *Biomaterials* **29**, 3306–3316. (doi:10.1016/j.biomaterials.2008.04.039)

Li, X. M., Gao, H., Uo, M., Sato, Y., Akasaka, T., Feng, Q. L., Cui, F. Z., Lui, M. H. & Watari, F. 2008*b* Effect of carbon nanotubes on cellular functions *in vitro*. *J. Biomed. Mater. Res. A.* (doi:10.1002/jbm.a.32203)

Li, X. M. *et al.* 2008*c* Maturation of osteoblast-like SaoS2 induced by carbon nanotubes. *Biomed. Mater.* **4**, 015 005. (doi:10.1088/1748-6041/4/1/015005)

Li, X. M., Lui, X. H., Dong, W., Feng, Q. L., Cui, F. Z., Uo, M., Akasaka, T. & Watari, F. 2008*d* *In vitro* evaluation of porous poly(L-lactic acid) scaffold reinforced by chitin fibers. *J. Biomed. Mater. Res. B.* (doi:10.1002/jbm.b.31311)

Liao, S., Wang, W., Uo, M., Ohkawa, S., Akasaka, T., Tamura, K., Cui, F. & Watari, F. 2005 A three-layered nano-carbonated hydroxyapatite/collagen/PLGA composite membrane for guided tissue regeneration. *Biomaterials* **26**, 7564–7571. (doi:10.1016/j.biomaterials.2005.05.050)

Liao, S., Watari, F., Zhu, Y., Uo, M., Akasaka, T., Wang, W., Xu, G. & Cui, F. 2007*a* The degradation of the three layered nano-carbonated hydroxyapatite/collagen/PLGA composite membrane *in vitro*. *Dent. Mater.* **23**, 1120–1128. (doi:10.1016/j.dental.2006.06.045)

Liao, S., Watari, F., Xu, G., Ngiam, M., Ramakrishna, S. & Chan, C. K. 2007*b* Morphological effects of variant carbonates in biomimetic hydroxyapatite. *Mater. Lett.* **61**, 3624–3628. (doi:10.1016/j.matlet.2006.12.007)

Liao, S., Ngiam, M., Watari, F., Ramakrishna, S. & Chan, C. K. 2007*c* Systematic fabrication of nano-carbonated hydroxyapatite collagen composites for biomimetic bone grafts. *Bioinspir. Biomim.* **2**, 37–41. (doi:10.1088/1748-3182/2/3/001)

Liao, S., Xu, G., Wang, W., Watari, F., Cui, F., Ramakrishna, S. & Chan, C. K. 2007*d* Self-assembly of nano-hydroxyapatite on multi-walled, carbon nanotubes. *Acta Biomater.* **3**, 669–675. (doi:10.1016/j.actbio.2007.03.007)

Lundqvist, M., Stigler, J., Elia, G., Lynch, I., Cedervall, T. & Dawson, K. A. 2008 Nanoparticle size and surface properties determine the protein corona with possible implications for biological impacts. *Proc. Natl Acad. Sci. USA* **105**, 14 265–14 270. (doi:10.1073/pnas.0805135105)

Matsuno, H., Yokoyama, A., Watari, F., Uo, M. & Kawasaki, T. 2001 Biocompatibility and osteogenesis of refractory metal implants, titanium, hafnium, niobium, tantalum and rhenium. *Biomaterials* **22**, 1253–1262. (doi:10.1016/S0142-9612(00)00275-1)

Matsuo, S., Watari, F. & Ohata, N. 2001 Fabrication of functionally graded dental composite resin post and core

by laser lithography and finite element analysis of its stress relaxation effect on tooth root. *Dent. Mater. J.* **20**, 257–274.

Moller, W., Felten, K., Kohlhaufl, M., Haussinger, K. & Kreyling, W. G. 2007 Motion and twisting of magnetic particles ingested by alveolar macrophages in non-smokers and smokers: implementation of viscoelasticity. *J. Magn. Magn. Mater.* **311**, 269–274. (doi:10.1016/j.jmmm.2006.10.1177)

Moller, W., Meyer, G. & Kreyling, W. G. 2008 Advances in lung imaging techniques for the treatment of respiratory disease. *Drug Discov. Today Ther. Strateg.* **5**, 87–92. (doi:10.1016/j.ddstr.2008.06.002)

Rosca, I. D., Watari, F. & Uo, M. 2004 Microparticle formation and its mechanism in single and double emulsion solvent evaporation. *J. Control. Rel.* **99**, 271–280. (doi:10.1016/j.jconrel.2004.07.007)

Rosca, I. D., Watari, F., Uo, M. & Akasaka, T. 2005 Oxidation of multiwalled carbon nanotubes by nitric acid. *Carbon* **43**, 3124–3131. (doi:10.1016/j.carbon.2005.06.019)

Sato, Y. *et al.* 2005*a* Strict preparation and evaluation of water-soluble hat-stacked carbon nanofibers for biomedical application and their high biocompatibility: influence of nanofiber-surface functional groups on cytotoxicity. *Mol. BioSyst.* **1**, 142–145. (doi:10.1039/b501222h)

Sato, Y. *et al.* 2005*b* Influence of length on cytotoxicity of multi-walled carbon nanotubes against human acute monocytic leukemia cell line THP-1 *in vitro* and subcutaneous tissue of rats *in vivo*. *Mol. BioSyst.* **1**, 176–182. (doi:10.1039/b502429c)

Smith, A. M., Duan, H., Mohs, A. M. & Nie, S. 2008 Bioconjugated quantum dots for *in vivo* molecular and cellular imaging. *Adv. Drug Deliv. Rev.* **60**, 1226–1240. (doi:10.1016/j.addr.2008.03.015)

Takagi, A., Hirose, A., Nishimura, T., Fukumori, N., Ogata, A., Ohashi, N. & Kanno, J. 2008 Induction of mesothelioma in p53+/− mouse by intraperitoneal application of multi-wall carbon nanotube. *J. Toxic. Sci.* **33**, 105–116. (doi:10.2131/jts.33.105)

Tamura, K., Takashi, N., Kumazawa, R., Watari, F. & Totsuka, Y. 2002 Effects of particle size on cell function and morphology in titanium and nickel. *Mater. Trans.* **43**, 3052–3057. (doi:10.2320/matertrans.43.3052)

Tamura, Y., Yokoyama, A., Watari, F., Uo, M. & Kawasaki, T. 2002*a* Mechanicalproperties of surface-nitrided titanium for abrasion resistant implant materials. *Mater. Trans.* **43**, 3043–3051. (doi:10.2320/matertrans.43.3043)

Tamura, Y., Yokoyama, A., Watari, F. & Kawasaki, T. 2002*b* Surface properties and biocompatibility of nitrided titanium for abrasion resistant implant materials. *Dent. Mater. J.* **21**, 355–372.

Uo, M., Watari, F., Yokoyama, A., Matsuno, H. & Kawasaki, T. 1999 Dissolution of nickel and tissue response observed by X-ray analytical microscopy. *Biomaterials* **20**, 747–755. (doi:10.1016/S0142-9612(98)00224-5)

Uo, M., Watari, F., Yokoyama, A., Matsuno, H. & Kawasaki, T. 2001*a* Tissue reaction around metal implants observed by X-ray scanning analytical microscopy. *Biomaterials* **21**, 677–685. (doi:10.1016/S0142-9612(00)00230-1)

Uo, M., Watari, F., Yokoyama, A., Matsuno, H. & Kawasaki, T. 2001*b* Visualization and detectability of rarely contained elements in soft tissue by X-ray scanning analytical microscopy and electron probe micro analysis. *Biomaterials* **22**, 1787–1794. (doi:10.1016/S0142-9612(00)00349-5)

Uo, M., Tamura, K., Sato, Y., Yokoyama, A., Watari, F., Totsuka, Y. & Tohji, K. 2005*a* The cytotoxicity of metal-encapsulating carbon nanocapsules. *Small* **1**, 816–819. (doi:10.1002/smll.200400143)

Uo, M., Asakura, K., Yokoyama, A., Tamura, K., Totsuka, Y., Akasaka, T. & Watari, F. 2005*b* Analysis of titanium dental implants surrounding soft tissue using X-ray absorption fine structure (XAFS) analysis. *Chem. Lett.* **34**, 776–777. (doi:10.1246/cl.2005.776)

Uo, M., Asakura, K., Kohgo, T. & Watari, F. 2006 Selenium distribution in human soft tissue determined by using X-ray scanning analytical microscope and X-ray absorption fine structure analysis. *Chem. Lett.* **35**, 66–67. (doi:10.1246/cl.2006.66)

Uo, M., Asakura, K., Yokoyama, A., Ishikawa, M., Tamura, K., Totsuka, Y., Akasaka, T. & Watari, F. 2007 X-ray absorption fine structure (XAFS) analysis of titanium-implanted soft tissue. *Dent. Mater. J.* **26**, 268–273. (doi:10.4012/dmj.26.268)

Ushiro, M., Uno, K., Fujikawa, T., Sato, Y., Tohji, K., Watari, F., Chun, W., Koike, Y. & Asakura, K. 2006 X-ray absorption fine structure (XAFS) analyses of Ni species trapped in graphene sheet of carbon nanofibers. *Phys. Rev. B* **73**, 144103-1–144103-11. (doi:10.1103/PhysRevB.73.144103)

Wang, W., Omori, M., Watari, F. & Yokoyama, A. 2005 Novel bulk carbon materials for implant by spark plasma sintering. *Dent. Mater. J.* **24**, 478–486.

Wang, W., Watari, F., Omori, M., Liao, S., Yokoyama, A., Uo, M. & Ohkubo, A. 2007 Mechanical properties and biological behavior of carbon nanotube/polycarbosilane composites for implant materials. *J. Biomed. Mater. Res. B Appl. Biomater.* **82b**, 223–230. (doi:10.1002/jbm.b.30724)

Watari, F. 2001 Compositional and morphological imaging of laser irradiated human teeth by low vacuum SEM, confocal laser scanning microscopy and atomic force microscopy. *J. Mater. Sci. Med.* **12**, 189–194. (doi:10.1023/A:1008913828931)

Watari, F. 2005 *In situ* quantitative analysis of etching process of human teeth by atomic force microscopy. *J. Electron Microsc.* **54**, 299–308. (doi:10.1093/jmicro/dfi056)

Watari, F., Yokoyama, A., Saso, F., Uo, M. & Kawasaki, T. 1997 Fabrication and properties of functionally graded dental implant. *Composites B* **28**, 5–11. (doi:10.1016/S1359-8368(96)00021-2)

Watari, F., Yokoyama, A., Omori, M., Hirai, T., Kondo, H., Uo, M. & Kawasaki, T. 2004 Biocompatibility of materials and development to functionally graded implant for bio-medical application. *Compos. Sci. Technol.* **64**, 893–908. (doi:10.1016/j.compscitech.2003.09.005)

Watari, F., Inoue, M., Akasaka, T., Sakaguchi, N., Ichinose, H. & Uo, M. 2006 Comparison of morphology and behavior of carbon nanotubes and asbestos. In *Proc. 6th Asian BioCeramics Symp.*, pp. 142–145.

Watari, F. *et al.* 2007*a* Biochemical and pathological responses of cells and tissue to micro- and nanoparticles from titanium and other materials. In *Handbook of biomineralization*, vol. 3 (ed. E. Bauerlein), pp. 127–144. Weinheim, Germany: Wiley-VCH.

Watari, F. *et al.* 2007*b* Effect of nanosizing of materials on living organism. In *Proc. Int. Symp. Nano Science and Technology (ISNST) 2007*, pp. 43–52. Tainan, Taiwan: Southern Taiwan University.

Watari, F. *et al.* 2007*c* Internal motion of micro/nano particles of titanium oxides and others in the body. *Archiv. BioCeramics Res.* **7**, 13–18. (*Proc. Asian BioCeramics Symposium* 2007.)

Watari, F., Abe, S., Tamura, K., Uo, M., Yokoyama, A. & Totsuka, Y. 2007*d* Internal diffusion of micro/nanoparticles inside body. *Bioceramics* **20**, 95–98. (Key engineering materials, vols. 361–363; *Trans. Tech. Publications*).

Watari, F. *et al.* 2008*a* Behavior of *in vitro*, *in vivo* and internal motion of micro/nano particles of titanium, titanium oxides and others. *J. Ceram. Soc. Jpn* **116**, 1–5. (doi:10.2109/jcersj2.116.1)

Watari, F., Inoue, S., Takashi, N., Totsuka, Y. & Yokoyama, A. 2008*b* Reaction of cells and tissue to material nanosizing. *Trans. Mater. Res. Soc. Jpn.* **33**, 209–214.

Watari, F., Yokoyama, A., Gelinsky, M. & Pompe, W. 2008*c* Conversion of functions by nanosizing—from osteoconductivity to bone substitutional properties in apatite. In *Interface oral health science 2007* (eds M. Watanabe & O. Okuno), pp. 139–147. Japan, Tokyo: Springer.

Watari, F. *et al.* 2009 Visualization of invasion into the body and internal diffusion of nanoparticles. *Bioceramics* **21**, 569–572. (Key engineering materials, vols. 396–398; *Trans. Tech. Publications.*)

Yokoyama, A. *et al.* 2005*a* Biological behavior of hat-stacked carbon nanofibers in the subcutaneous tissue in rats. *Nano Lett.* **5**, 157–161. (doi:10.1021/nl0484752)

Yokoyama, A., Gelinsky, M., Kawasaki, T., Kohgo, T., Konig, U., Pompe, W. & Watari, F. 2005*b* Biomimetic porous scaffolds with high elasticity made from mineralized collagen—an animal study. *J. Biomed. Mater. Res. Appl. Biomater.* **75b**, 464–472. (doi:10.1002/jbm.b.30331)

Zhu, Y. & Watari, F. 2007 Surface carbonization of titanium for abrasion-resistant implant materials. *Dent. Mater. J.* **26**, 245–253. (doi:10.4012/dmj.26.245)

JOURNAL OF THE ROYAL SOCIETY Interface

JOURNAL OF THE ROYAL SOCIETY Interface

ナノマテリアルの生体反応
リスクと活用

亘理文夫
Fumio WATARI
北海道大学大学院歯学研究科教授

1 ナノマテリアルの2面性：リスクと高機能性

抗がん剤は，しばしばがん患部に到達する前に健常組織に吸収され副作用に働いてしまう．この欠点を回避するために，ドラッグデリバリーシステム(DDS)は，薬剤に標的患部にのみ特異的に結合する修飾基を付け血流中を移送し選択的に投与するシステムであり，ナノマテリアルの代表的なバイオ応用例として抗がん剤投与や遺伝子導入に開発が期待されている．

一方，生体親和性に優れるチタン[1]は摩耗粉[2,3]では炎症を引き起こし，粘土鉱物の1種アスベスト[4]は長期大量に被曝すると中皮腫を発症する．ここには，マクロでの材料特性は生体親和性を有していてもミクロ/ナノになると為害性に作用するという，ある種の機能性転換が見られる．こうした現象には，単にマクロで現れる材質が毒性か生体親和性かという特性とは別に，微粒子に起因する効果[5~11]が寄与していると考えられる．ナノテクノロジーの進展とともにナノ物質の開発が進行し，新しい機能性や高効率性が実現されつつあるが，一方，ナノサイズ化により化学反応は著しく促進されることから，メリット(高機能性)とともに，意図せずしてデメリット(為害性)もまた昂進されることも十分に可能性がある．ナノテクノロジーの人体へのバイオ応用には，あらかじめミクロ/ナノ微粒子の生体反応性に関する適切な理解と指針が必要である．

本稿では，材料がマクロからミクロ/ナノサイズ化(以下，ナノサイジングと総称)したときに起きる生体反応を概括する．

2 ナノサイジング効果(1)：溶出性材料と比表面積効果

毒性発現にせよ栄養摂取にせよ，材料に対する生体の反応の多くは水溶性のイオンとして溶出し体内に取込まれることから開始する．例えばフグにせよトリカブトにせよ，急性毒性を示す物質は水溶性である．ナトリウム(Na)のような1価の金属塩は一般に可溶性であり，そのため塩分は摂取過剰になりがちであるのに対し，難溶性の2価塩であるカルシウム(Ca)は摂取不足になりやすい．このように，マクロでの材料の生体適合性には溶出性(だけではない)が，大きな影響を及ぼす．この傾向はミクロ/ナノになっても変わらず，微粒子になりサイズが小さくなると比表面積は増大するから，溶解性や化学反応性は著しく増大する．

ナノサイジング効果は通常，この化学反応昂進を引き起こす比表面積増大効果で説明される．図1は溶出性で為害性を有する材料の代表例としてニッケル(Ni)を，非溶出性で親和性に富む材料の代表としてチタン(Ti)を取り上げ比較したもので，0.5 μmの微粒子に対するヒト好中球の反応を走査型電子顕微鏡(SEM)像で示している．[7,8] マクロサイズの場合，皮膚接触でアレルギー性を示すNiを体内軟組織に埋入すると，Ni近傍の組織は壊死し遠隔領域

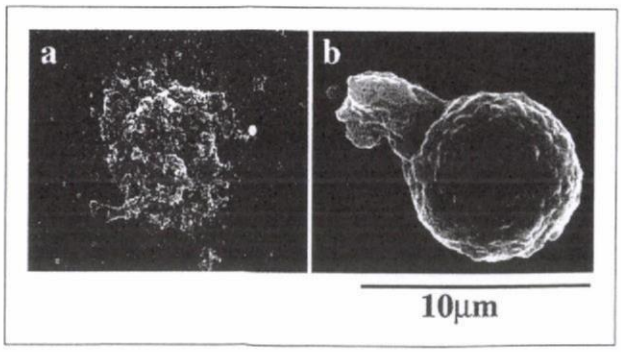

図1 0.5 μm Ni(a)及び0.5 μm Ti(b)微粒子に対するヒト好中球の反応(SEM像)
溶出性で為害性を有するNiでは細胞は破壊に至り，非溶出性で親和性に富むTiではその粒子サイズが貪食を誘発する．[8]

でも強い炎症を示す．こうした領域は，Niのイオン溶出領域と一致することが示される．[12] Niを0.5 μmの微粒子にし，細胞と培養液中で共在させると細胞は破壊され(図1a)，さらにラットの軟組織中に長期(半年～1年間)大量に埋入すると腫瘍を発生する．[5] この現象は，マクロでの効果がミクロ/ナノで著しく増進する比表面積効果の1例である．

3 ナノサイジング効果(2)：非溶出性材料と物理的サイズ効果

一方，マクロサイズのTiは生体親和性に優れインプラントに用いられるが，微粒子になると図1bのように貪食を誘発する．このとき，Ti粒子からのイオン溶出を誘導結合プラズマ発光分析装置(ICP-AES)で分析すると，検出限界値以下であり，イオン溶出は無視できる．[7,8] すなわち，図1bの貪食はイオン溶出という化学的効果ではなく，物理的粒子サイズそのものが貪食を誘発しているのである．

図2は，図1と同じ条件下でTi，TiO_2微粒子と共在させたヒト好中球から産生した代表的な炎症性サイトカインTNF-α量の微粒子サイズ依存性を示したものである．[5] 粒子サイズが，150～0.5 μmへ順次小さくなるにつれ放出量は増加する傾向にあるが，とりわけ10 μm以下で急激に増加する．*In vitro*, *in vivo* 試験の結果を総合すると，100 μm以上では巨視的サイズと同様の親和性を示すが，[7] 50 μm以下では刺激性が増加し，10 μm以下になると貪食作用を誘発し(図1b)，0.5～1 μm前後で最も刺激性が昂進し(図2)，炎症を引き起こす．この現象は金属，セラミックス，ポリマーの材料に依存せず，非溶出性材料やbioactive，bioinert材料共通に起きる．図2で同一サイズのTi，TiO_2粒子がほぼ同等レベルのTNF-α産生を示しているのは，その1例である．

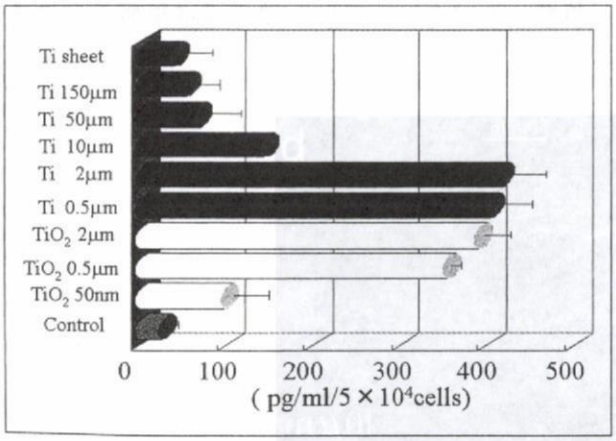

図2 炎症性サイトカインTNF-α産生のナノサイズ領域までの微粒子サイズ依存性[5]

この刺激性は細菌内毒素に比べると1/1,000～1/10,000程度であり，[13,14] 少量・短期的であれば特に問題はないと思われる．しかし大量・長期間にわたる場合には，慢性的に貪食・炎症を継続するため注意が必要である．例えば人工関節にTiを用いた場合，骨頭摺動部から発生した摩耗粉が炎症を引き起こし骨融解を導き人工関節の寿命が10年程度に終わる場合や，組成的には粘土鉱物の1種アスベストは長期大量に被曝すると中皮腫を発症する現象は，単に毒性か生体親和性かという特性や比表面積効果では理解できず，微粒子の物理的サイズ・形状が誘発し慢性的な炎症に移行する上記の刺激性が発症の背景となっている．

4 生物学的プロセスによる機能性転換

これらナノサイジングが誘発する生体反応は炎症を引き起こし，しばしばサイトカイン放出，細胞の分化誘導等の様々な生体反応のなかから，材料の置かれた状況に応じて生起した生物学的プロセスを通し，機能性転換を示現する．マクロで生体親和性を示すTiが，摩耗粉では炎症を誘発する現象やアスベストによる中皮腫発症はマクロでの親和性からミクロ/ナノでの為害性に機能性転換する例であり，さらに以下がある．

5 ナノアパタイトの骨置換性転換

アパタイトは生体親和性に富み，優れた骨伝導性を示すが，それ自体は骨に置き換わらない．そのため，インプラント材料として使用される．図3は，アパタイトコーティングチタンからなるデンタルインプラント(人工歯根)の失敗例を示したものである．[15] 親和性に優れたアパタイトといえども，微細

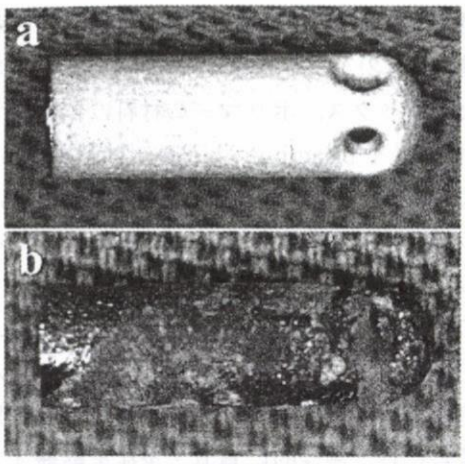

図3　アパタイトコーティングチタンデンタルインプラント

a：装着前，b：失敗例．アパタイトなどの微細なダストは貪食・炎症を誘発し，新生骨と被覆アパタイトの吸収を生じ動揺・脱落に至る．

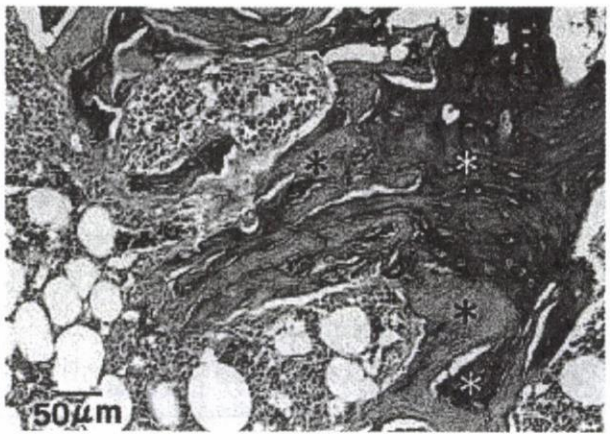

図4　ナノアパタイト–コラーゲンコンポジットの骨置換性

ナノコンポジット部(黒＊)の吸収と新生骨形成(白＊)が不可分に生じ，結果として骨置換性が達成されている．[16]

なダストを発生すると貪食・炎症を誘発し新生骨と被覆アパタイトの吸収を導き，動揺・脱落して失敗に至る．これもやはり親和性から為害性への機能性転換の例である．

しかし我々の天然骨は約50 nmのナノアパタイトからなり，リモデリングにより骨吸収と形成のプロセスを繰返している．図4は天然骨を模倣し作製したナノアパタイト–コラーゲン/コンポジットを骨欠損部に埋入した場合の組織像で，破骨細胞によるナノコンポジット部(黒＊)の吸収と骨芽細胞による新生骨形成(白＊)が同時・隣接して不可分に生じ，経時的に進行することにより結果として骨置換性が達成されている．[16] ここには，マクロにおけるアパタイトの非骨置換性からナノにおける骨置換性への機能性転換が起きている．[17]

6　カーボンナノチューブ(CNT)の細胞付着性転換

元素としての純炭素の生体適合性はNiのような為害性はないが，アパタイトのような生体活性(bioactive)やTiほどの親和性はなく，生体不活性(bioinert)と考えられる．図5は，同じ純炭素の同素体(多形)であるグラファイト(黒鉛)(a)とCNT(b)に対する骨芽細胞様細胞(Saos 2)の接着性を示したものである．結晶構造は，ともに炭素の六員環が2次元に配列したグラフェンシートからなり，マクロなグラファイトではグラフェンシートが平面状に積層しているのに対し，CNTでは単層または多

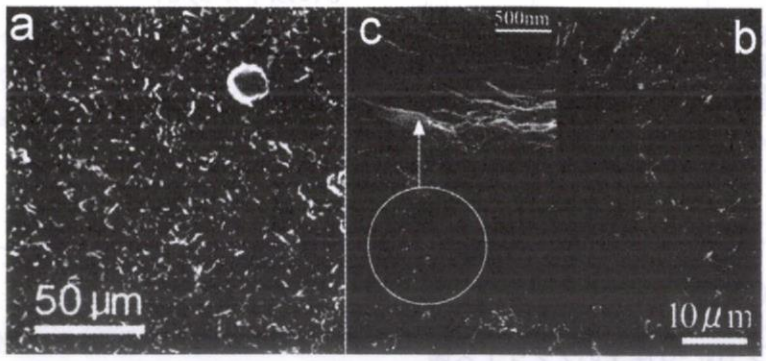

図5　グラファイト(a)とCNT(b)に対する骨芽細胞様細胞の付着性

層のグラフェンシートがナノサイズの直径の円環状に閉じたチューブ状をなしている.[18,19] グラファイト(a)には細胞がほとんど付着しないのに対し,CNT上(b)では付着・伸展し細胞末端から多数の長く延伸した直径約100 nmの糸状仮足がCNT叢と結合している(c).[20,21] 細胞非付着性のグラファイトはその抗血栓性により人工心臓弁に使用されるが,CNT上では細胞と強く付着し,ナノサイジングにより非細胞接着性から細胞接着性に機能性転換している.この強い細胞接着性の発現には,CNT表面への蛋白質吸着[20,22,23]による細胞親和性の向上と,糸状仮足が相互作用しやすい直径数nm～数10 nmのナノネットワーク構造の組成的及び幾何学的効果が寄与している.

7 ナノ微粒子の体内侵入・全身拡散と薬剤の体内動態

この材料に非特異的な物理的微粒子サイズに由来する刺激性は,マイクロメートル近傍で最大値を示した後,更に微小なナノメートル領域になるとむしろ低下する(図2).[5] ナノ物質の応用の観点からは一見都合がよさそうに見えるが,別の見方をすれば異物に対する生体の認識能力あるいは防御能力が低下するということにも通ずる.微粒子の大きさが約10 μmを切ると気管支を通過するが,図6は化粧品に使われている30 nmのTiO_2粉末をラットに強制曝露したときの体内侵入・全身分布像である.これは収束X線プローブを照射し,試料から発光した蛍光X線をマッピングするX線走査型分析顕微鏡

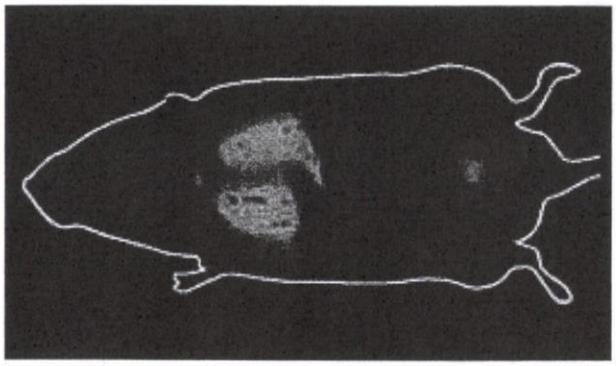

図6 呼吸器系からのナノ微粒子の体内侵入/全身拡散:30 nmTiO_2粒子の強制曝露試験後のXSAMマッピングによるラット体内の全身Ti元素分布像[5]

(XSAM)[12]により得られたTi元素分布像である.[5] 呼気に乗って肺胞に到達したナノ粒子が肺から直接血中に取り込まれ,全身に拡散することが分かる.経口投与試験でも濃度は低いが,脾臓等からTiが検出され,消化器系からも体内侵入・全身拡散することが示される.[24] これらの体内動態は,意図せずして体内侵入し為害性をなし得るというデメリットとして捉えられるが,逆の観点からいえば薬剤投与後の体内動態そのものであり,DDSの標的患部への移送プロセスというナノテクの活用のメリットとしての意義にも該当する.

図7は体内動態をより簡便に調べるために,マウスの尾静脈から直接血流に投与した結果で,XSAM-Ti元素マッピングによるTiO_2の投与直後,3時間,1日後の分布を示している.血流に乗った30 nmTiO_2粒子は,投与直後まず心臓に戻った後,肺

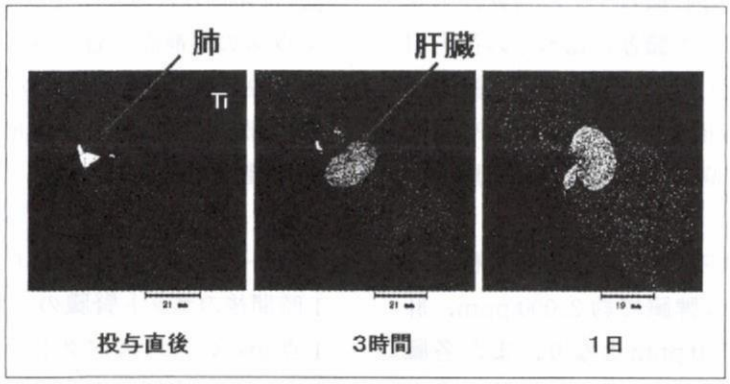

図7 XSAM-Ti元素マッピングによるマウス尾静脈注入後のTiO_2粒子(30 nm)の全身動態[24]

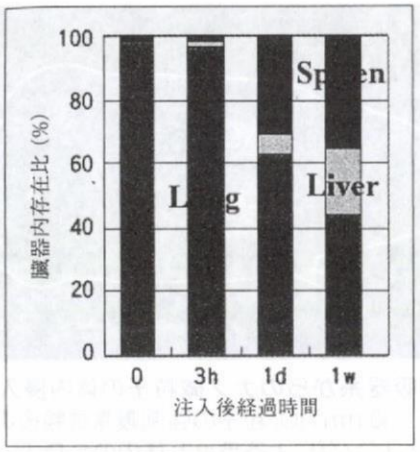

図8　TiO_2粒子の各臓器への相対的存在比の経時的変化[10]

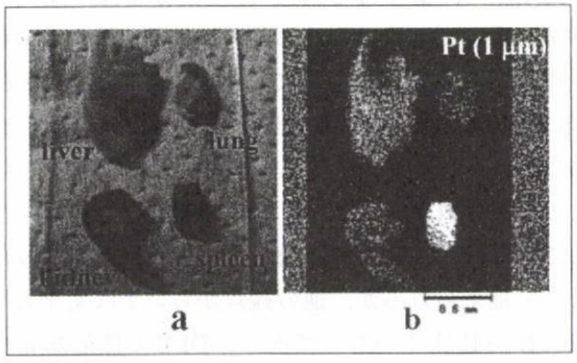

図9　Pt微粒子投与1日後のマウス各臓器(a)のPt元素マッピング像(b)[25]

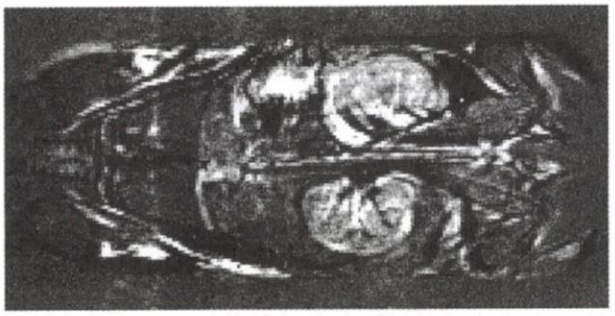

図10　マグネタイト粒子(11nm Fe_3O_4)を尾静脈注入したマウスの投与前，投与1週後のMRI差画像[25]

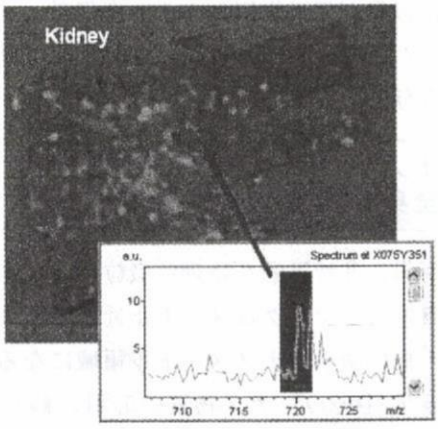

図11　水溶化フラーレン投与1時間後のラット腎臓のC_{60}レーザーマス・マッピング像(左)と，腎臓内1点からのマススペクトル(右)[25]

に到達し，数時間～数週間かけて肝臓，さらに脾臓に拡散移行する．図8はTiO_2粒子の各臓器への相対的存在比の経時的変化を示したもので，肺→肝臓→脾臓と順次臓器間移行している．[24]

図7，8のような経路を経て体内拡散するタイプの材料とは異なり，白金(Pt)微粒子では当初から脾臓に優先的に捕捉され，他の臓器に比べその後も引続き滞留している比率が高い．図9は，Pt微粒子投与1日後のマウスから摘出した各臓器のPt元素マッピング像で，脾臓で高濃度に検出され，肝臓がこれに次ぐ．

これらの臓器をICP-AESで分析し定量解析すると，各臓器中のPt濃度は脾臓で約2,000 ppm，肝臓で700 ppm，腎臓は<50 ppmとなり，また各臓器内に含まれるPt総量は体積の大きい肝臓で最も多く，初期投与量の約25%が肝臓に，次いで5%が脾臓にトラップされ，その他の臓器も含めれば40%近くが臓器で検出されたことになる．血流に乗った微粒子の相当程度が臓器に捕捉されていることが分かる．[25]

図10は，がんのハイパーサーミア治療(温熱療法)に用いられるマグネタイト粒子(11 nm Fe_3O_4)をマウスの尾静脈へ注入後，MRI撮像し画像処理により投与前，投与1週後の差画像としたもので，高濃度部が呈する白色コントラストから，腎臓への濃縮が確認できる．

図11は，レーザーアブレーション/マススペクトル(レーザー・マス)法による水溶化フラーレン投与1時間後のラット腎臓のイメージング像で，腎臓内1点からのマススペクトル(右)にはC_{60}(M＝720)付近にピークが認められ，そのマッピング像(左)がフラーレンの臓器内分布を表示している．フラーレン

Interface Oral Health Science 2007: 139–148

Conversion of functions by nanosizing—from osteoconductivity to bone substitutional properties in apatite

Fumio Watari[1]*, Atsuro Yokoyama[1], Michael Gelinsky[2], Wolfgang Pompe[2]
[1]*Graduate School of Dental Medicine, Hokkaido University, Sapporo 060-8586, Japan;*
[2]*Max Bergmann Center of Biomaterials, Institute of Materials Science, Technical University, 01069 Dresden, Germany*
*watari@den.hokudai.ac.jp

Abstract. Synthetic hydroxyapatite, in the usual case, of a macroscopic size, exhibits excellent osteoconductivity. However, it is not substituted with natural bone and remains permanently in the body; therefore it is suitable for using as an implant. It is well known that natural bone is composed of collagen and nanocrystallites of apatite with the size of approximately 50 nm. When the composite with collagen and nanoapatite synthesized in the biomimetic aspects is implanted, phagocytosis and inflammation are induced. Osteoclasts and osteoblasts are then differentiated and activated. The bone resemblant material and its phagocytizable nanometer size provide the conditions that composite is biologically degradable through phagocytosis by osteoclasts, and new bone formation by osteoblasts is simultaneously activated and proceeded. As a result, nanocomposite leads to the bone substitutional properties. Thus the conversion of functions is attained for apatite by nanosizing—from osteoconductivity in macroscopic size to bone substitutional properties in nano/micro scale. This tendency is more enhanced for carbonated hydroxyapatite. The mineralization surrounding collagen fibrils determines the crystallization of apatite for their size and orientations. Nanoparticles cause the reaction of cells/tissue and stimulate the occurrence of inflammation, which works as a stimulus in most cases or pronounces the conversion of functions leading to the bioactive properties for some cases, depending on the situation. Nano structure is essential for these stages to be processed.

Key words. nanosizing, apatite, tissue regeneration, inflammation, nanotoxicology

Introduction: non-resorbable and resorbable apatite

Synthetic hydroxyapatite in the usual case, that is, in a macroscopic size, exhibits excellent osteoconductivity. However, it is not substituted for natural bone and remains permanently in the body; therefore it is suitable for using as an implant.

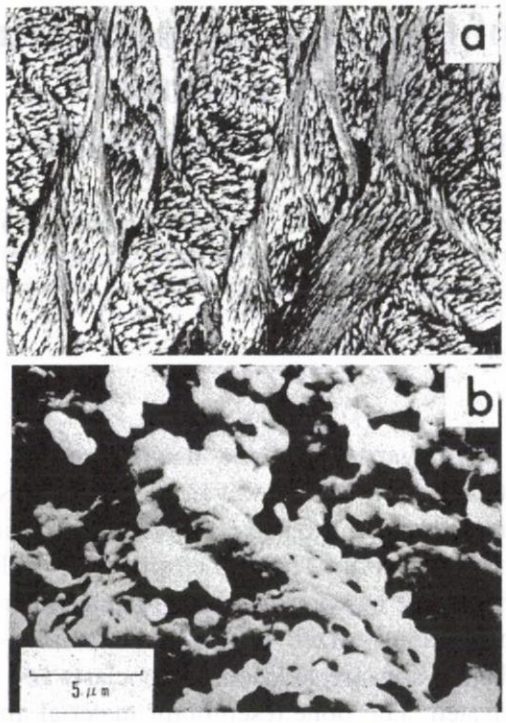

Fig. 1. Difference of morphology of hydroxyapatite. **a** Enamel of molar of rat, **b** sintered synthetic apatite

It is well known that natural bone is composed of collagen and nanocrystallites of apatite with the size of approximately 50 nm. In Fig. 1 the SEM photographs compare the difference in morphology of hydroxyapatite for natural hard tissue, in this case, enamel of molar of rat (a) and sintered synthetic apatite (b). In synthetic apatite the size of particles is a few microns, and they agglomerate in random, while in enamel, enamel prism of about 5 μm is composed of a bunch of apatite crystallites of about 50 nm. It is known that apatite crystallites are grown in their *c*-axis along collagen fibrils. Thus natural hard tissue is regarded as a kind of composite with the preferably oriented structure of nanocrystallites.

There is the difference in behavior between synthetic apatite and bone. Bone is continuously remodeled by resorption and new bone formation. Thus there exist apatites with different behaviors, non-resorbable and resorbable apatites. The problem arises: what is their difference and its cause? We will first see the nanosizing effect in general, and then the case of apatite and its mechanism.

Materials and methods

Both biochemical cell functional tests and animal implantation tests were done to investigate the reaction to fine particles of 99.9% pure Ti, Fe, Ni, and TiO_2 for the various sizes from 300 nm to 150 μm [1]. Human neutrophils were used as probe

cells for various cell toxicity tests, after mixed with particles in Hank's balanced salt solution (HBSS) at 37°C. Histological investigations were done after implanting in the subcutaneous connective tissue of rats.

Hydroxyapatite-collagen composites were synthesized biomimetically on mineralized collagen type I. They have the three-dimensional scaffold structures with the interconnecting pores. They were implanted into the subcutaneous tissue, and bone defects made in the femur of rats for 1–12 weeks and observed histopathologically [2].

Results

Micro/nanosizing effect onto cell/tissue reaction

Figure 2 shows the dependence of TNF-α release from human neutrophils on the size of Ti particles. TNF-α was increased with the decrease in particle size. The increase was pronounced for 0.5 and 3 μm. The release of LDH, superoxide and cytokine Il-1β showed the similar behavior as TNF-α, while cell survival rate showed the inverse decreasing tendency. Under these conditions ICP elemental analysis indicated that the dissolution from Ti particles was negligible below detection limit [1].

Figure 3 shows the SEM image of human neutrophils of control (a) and the one exposed to 0.5 μm Ti particles (b) where a neutrophil extends its pseudopod to phagocytize Ti particles for the size less than 10 μm [3]. For the particles larger

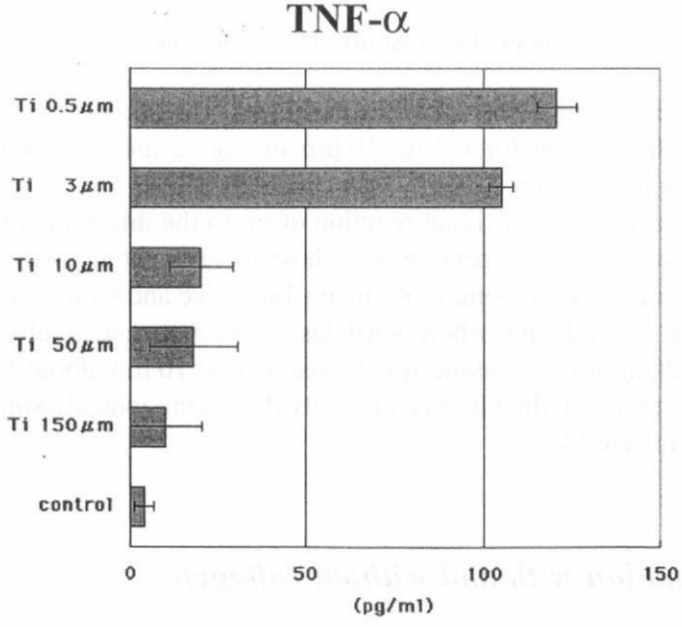

Fig. 2. Dependence of TNF-α release from human neutrophils on Ti particle size [1]

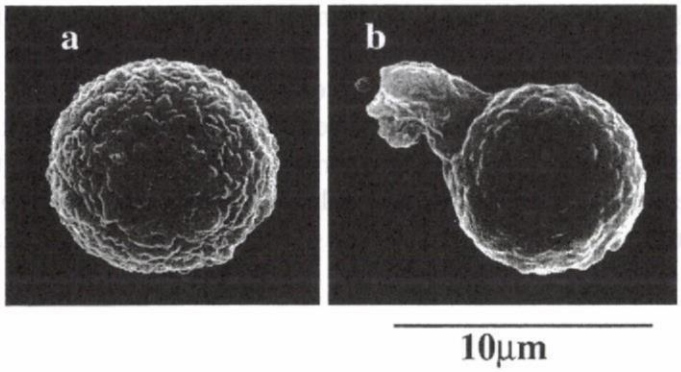

Fig. 3. SEM images of human neutrophils. **a** Control, **b** exposed to particles of Ti (500 nm) [3]

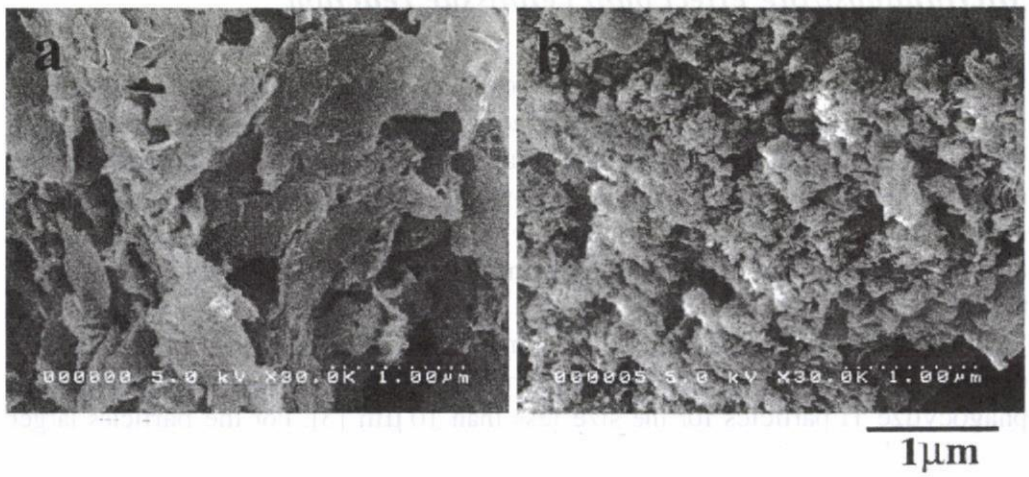

Fig. 4. Hydroxyapatite synthesized without (**a**) and with (**b**) collagen

than about 10 μm, phagocytosis was not observed. The pronounced phenomena of biochemical cell reaction for below 10 μm in Fig. 2 are closely related to the phagocytosis shown in Fig. 3.

The histological image of tissue reaction of rat to the different sizes of Ti particles showed a similar size dependence to those in vitro shown in Figs. 2 and 3.

These phenomena occur commonly in any bioactive and bioinert materials other than Ti, such as Fe and TiO_2 where particles induce non-specifically phagocytosis to cells and inflammation to tissue for the size below 10 μm, about the cell size. It is different from the usually observed toxicity due to the ionic dissolution effect in the macroscopic size [4].

Apatite formation with and without collagen

Figure 4 shows the comparison of morphology of hydroxyapatite synthesized without (a) and with (b) collagen by SEM observation. The particle size of

apatite is mostly a few microns for without-collagen, while under the coexistence of collagen the product becomes the agglomerate of apatite crystallites of less than 100 nm with the lower crystallinity, revealed from X-ray diffraction analysis.

Failure of dental implants by bone desorption

In clinical cases of dental implants, failure sometimes occurs. Figure 5 shows the example of hydroxyapatite-coated titanium implant: before (a) and after (b) implantation. Failure occurs through inflammation and the resorption of apatite and the surrounding alveolar bone. Inflammation is induced by various reasons. The breakage of apatite-coating film or release of fine dust of apatite powders is one of the causes.

Resorption of nanoapatite and simultaneous osteogenesis in bone circumstances

When the biomimetic nanocomposites of apatite and collagen fibrils were implanted in the subcutaneous tissue, they were covered with fibrous connective tissue and then resorbed mostly at 8 weeks by phagocytosis.

Figure 6 shows the histopathological image when they were implanted in the bone marrow of rat for 8 weeks [2]. The area of nanocomposites (asterisks) was decreased and covered with new bone (white asterisks) of lamellar structures. Resorption of the nanocomposites and replacement by new bone proceeded. This tendency was progressed with time by 12 weeks. As shown in Fig. 6, phagocytosis

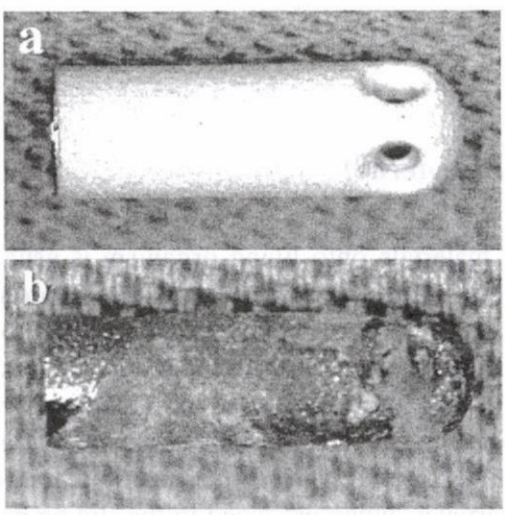

Fig. 5. Example of failure of dental implant of apatite-coated titanium: before (**a**) and after (**b**) implantation

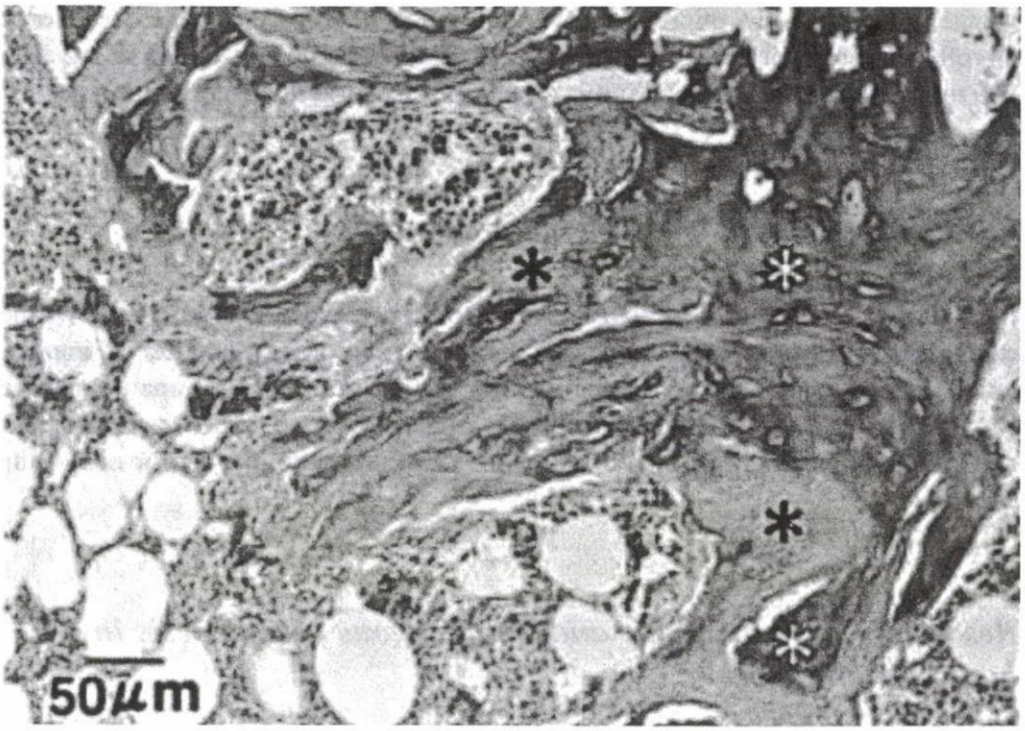

Fig. 6. Histology at 8 weeks after implantation in the bone marrow of rat. Materials (*asterisks*) were decreased and covered with new bone (*white asterisks*) with lamellar structures. AZ stain [2]

of nanoapatite by osteoclasts and osteogenesis by osteoblasts occurred adjacently to each other. Resorption and remodeling were similar to the case of autologous bone graft. As a result nanoapatite composites work as bone substitute materials for hard-tissue reconstruction.

Discussion

Nanosizing effect (general)

Nanosizing effect of materials onto living organism is usually interpreted as the aspects of the increase in specific surface area, which pronounces the chemical reactivity with the decrease in particle size. Effects related to the ionic dissolution correspond to this category, such as the acceleration of toxicity observed in Ni where tumor was generated in the long-term implantation for 0.5 μm particles [4], compared with necrosis that occurred in short term for macroscopic size [5]. There are, however, other kinds of effects [4]. Biocompatible titanium causes inflammation in abraded fine particles, when produced in the sliding parts of artificial joints, and asbestos [6], a kind of clay mineral, induces mesothelioma after a long

term, large quantity of exposure. They can be understood as the physical particle effect, apart from the chemical material properties of either toxicity or biocompatibility.

Figure 2 showed clearly the cytotoxicity due to fine particles and its size dependence. Cytotoxicity and inflammation were pronounced when the particle size was smaller than 10 μm, about the cell size, where phagocytosis was induced.

Bioactive properties induced by nanosizing

Specific surface area effect is based solely on the material properties, and material-dependent, whereas the physical particle size effect has the origin in the relative size relationship between particles and cell/tissue and independent of materials. Stimulus arises as non-specific events to any bioinert, bioactive materials of metals [7], ceramics, polymers by biological process, which induces the occurrence of functionality of body defense system.

The term "biocompatible" may be classified into two categories: "bioinert" and "bioactive". "Bioinert" may be used for the materials which give neither harmful effects nor positive functional effects. Alumina, carbon, and Ti may also be included in this category. "Bioactive" is used for the materials which induce the intrinsic functional effects of the living organism, usually in a positive sense, for example, apatite inducing osteoconductivity.

The judgment of positive or negative is based on the evaluation system in the application for human beings whether they work usefully or obstructively, and indifferent from their generation mechanism. If we enlarge the definition of "bioactive" as the potential properties to induce the intrinsic functional effects of the living organism, including both the positive and negative sense, nanosizing effect can be classified as bioactive whether it generates inflammation or osteogenesis.

Nanosizing induces the non-specific phagocytosis of particles, which gives rise to the superoxide production, cytokine emission and differentiation/activation of cells which lead to inflammation in tissue.

Nanosizing effect in apatite

In the case of apatite, nanosizing effect induces phagocytosis and leads to the apparent inflammation, which causes bone resorption in some cases like Fig. 5 and bone formation in other cases like Fig. 6, depending on the bone circumstances of these events. The former causes the failure of dental implants where the hydroxyapatite-coating film on titanium implant and the surrounding newly formed bone were resorbed. The breakage of apatite-coating film and release of fine dust of nanoapatite powders could be one reason to activate osteoclasts and other phagocytizing cells. The similar phenomena are also well known for other materials. For

example, abrasion particles produced from the sliding parts of artificial joints cause inflammation, whether material is polymer (polyethylene, etc.), metal (Ti, Co–Cr) or ceramics (alumina), and lead to osteolysis in the surrounding bone tissue, which determines the lifetime of using artificial joints.

When nanoapatite-collagen composites [2] or their derivatives reinforced with PLA or PLGA [8] were implanted into the bone defects of hard tissue, it leads apparently to the inflammation where cytokine emission and the differentiation or activation of osteoclasts and osteoblasts occur. Then the phagocytosis of nanoapatites by osteoclasts and osteogenesis by osteoblasts occur adjacently to each other, and the resorption of nanoapatite composites and new bone formation proceed simultaneously with time as shown in Fig. 6. As a result nanoapatite composites are substituted with new bone. Thus nanoapatite induces bioactive functions and works as bone substitutional. This tendency is more enhanced for carbonated hydroxyapatite. These phenomena are very similar to the bone remodeling process which occurs in natural bone.

Conversion of functions by nanosizing

Apatite in macroscopic size works as osteo-conductive but non-bone substitutional, while nano-size apatite works as bone substitutional.

Here, there is a conversion of functions of materials by nanosizing—from osteo-conductivity to bone substitutional properties in apatite.

Stimulus and bioactive properties of nanomaterials induced by biological process

Nanosizing causes the reaction of cells/tissue and stimulates to the occurrence of inflammation, which works as the stimulus in most cases. This toxicity is very weak compared with endotoxin [4]. Inflammation generates the conversion of functions leading to the bioactive functions for some cases, depending on the situation. These stimuli are different from those by specific surface effect where origin is solely from materials.

Conclusions

Synthesized hydroxyapatite, usually in macroscopic size, is osteoconductive but non-bone substitutional. Nanosizing of apatite induces bioactive reactivity to tissue where bone resorption or bone substitutional functions arise through the expression of inflammation, depending on the circumstances. Adjacent occurrence of resorp-

tion of nanoapatite composite by osteoclasts and simultaneous new bone formation by osteoblasts is very similar to the remodeling process of natural bone. Nanosizing works as a bioactive and causes inflammation, which leads to the conversion of functions through biological process such as from biocompatible to stimulative or from osteoconductive but non-bone substitute to bone substitute. Thus nanosizing of apatite is essential for hard tissue reconstruction and bone remodeling in the living organism.

Acknowledgments. The present study was performed under the support of Health and Labour Sciences Research Grants in Research on Chemical Substance Assessment from the Ministry of Health, Labour and Welfare of Japan (H18-Chemistry-General-006).

References

1. Tamura K, Takashi N, Kumazawa R, et al (2002) Effects of particle size on cell function and morphology in titanium and nickel. Mater Trans 43:3052–3057
2. Yokoyama A, Gelinsky M, Kawasaki T, et al (2005) Biomimetic porous scaffolds with high elasticity made from mineralized collagen—an animal study. J Biomed Mater Res Part B Appl Biomater 75B:464–472
3. Kumazawa R, Watari F, Takashi N, et al (2002) Effects of Ti ions and particles on cellular function and morphology of neutrophils. Biomaterials 23:3757–3764
4. Watari F, Tamura K, Yokoyama A, et al (2007) Biochemical and pathological responses of cells and tissue to micro- and nanoparticles from titanium and other materials. In: Bauerlein E (ed) Handbook of biomineralization, vol 3. Wiley-VCH, Weinheim, pp 127–144
5. Uo M, Watari F, Yokoyama A, et al (1999) Dissolution of nickel and tissue response observed by X-ray analytical microscopy. Biomaterials 20:747–755
6. Watari F, Inoue M, Akasaka T, et al (2006) Proceedings of the 6th Asian bioceramics symposium 2005, pp142–145
7. Matsuno H, Yokoyama A, Watari F, et al (2001) Biocompatibility and osteogenesis of refractory metal implants, titanium, hafnium, niobium, tantalum and rhenium, Biomaterials 22:1253–1262
8. Liao S, Wang W, Uo M, et al (2005) A three-layered nano-carbonated hydroxyapatite/collagen/PLGA composite membrane for guided tissue regeneration. Biomaterials 26:7564–7571

Key Engineering Materials Vols. 396-398 (2009) pp 569-572
online at http://www.scientific.net

Online available since 2008/Oct/21

Visualization of invasion into the body and internal diffusion of nanoparticles

F.Watari[1, a], S.Abe[1], I.D.Rosca[2], A.Yokoyama[1], M.Uo[1], T.Akasaka[1], N.Takashi[1], Y.Totsuka[1], E.Hirata[1], M.Matsuoka[1], K.Ishikawa[1], S.Itoh[1] and Y.Yawaka[1]

[1]Graduate School of Dental Medicine, Hokkaido University, Sapporo 060-8586, Japan

[2]Mechanical & Industrial Engineering, Concordia University, Montreal, Quebec H3G1M8, Canada

[a]watari@den.hokudai.ac.jp

Keywords: nanoparticle, internal diffusion, nanotoxicology, size effect, DDS, mapping.

Abstract. Nanoparticles may invade directly into the internal body through the respiratory or digestive system and diffuse inside body. The behavior of nanoparticles in the internal body is also essential to comprehend for the realization of DDS. Thus it is necessary to reveal the internal dynamics for the proper treatments and biomedical applications of nanoparticles. In the present study the plural methods with different principles such as X-ray scanning analytical microscope (XSAM), MRI and Fluorescent microscopy were applied to enable the observation of the internal diffusion of micro/nanoparticles in the (1) whole body level, (2) inner organ level and (3) tissue and intracellular level. Chemical analysis was also done by ICP-AES for organs and compared with the results of XSAM mapping.

Introduction

Particles of the size below 200nm may invade directly into the internal body through the respiratory or digestive system and diffuse inside body. Nanoparticles might be the objects whose existence has not been assumed by living body defense system [1]. Thus the visualization of the internal dynamics of nanoparticles is essential for the proper treatments based on risk assessment and biomedical applications such as DDS (Drug delivery System). In the present study plural methods with different principles were applied to enable the observation of the internal diffusion of micro/ nanoparticles in the (1) whole body level, (2) inner organ level and (3) tissue and intracellular level.

Materials and Methods

1. Visualization of Internal Particle Diffusion in the Whole Body Level. The compulsory exposure test to the respiratory system was performed to rats using 30 nm TiO_2 particles. The uptake of nanoparticles through the digestive system was also tested for mice by mixing agar gelatin containing 30 nm TiO_2 particles to their foods. To inspect internal diffusion more simply, the experiments were done for mice by injecting nanoparticles directly into the cardiovascular system at caudal vein. The observation of internal distribution of nanoparticles was conducted for the whole body and each organ by elemental mapping in air using X-ray Scanning Analytical Microscope (XSAM: Horiba XGT-2000V, Tokyo, Japan) without staining [2,3]. The experiments were also done for the particles Ti, Fe, Ni, Pt, TiC, Fe_3O_4, Fe_2O_3 and carbon nanotubes [4,5]. Chemical analysis was done by ICP-AES (Inductively Coupled Plasma - Atomic Emission Spectrometry) for organs and compared with the results of XSAM mapping.

Three-dimensional and chronological observation by MRI (Magnetic Resonance Imaging) was done for the 11 nm magnetite Fe_3O_4 particles, using the MRI with the magnetic field strength 7 Tesla for animal experiment (Varian Co.Lmd) under the conditions of TR/TE 5000/20 ms, matrix 256 x 128, FOV 80 x 40 mm^2, slice thickness 1mm. The results were compared with those taken by XSAM.

2. Visualization in the Inner Organ Level. Fluorescent microscopic method was also applied to detect the internal distribution using the fluorochrome-labeled particles. The fluorescent dye,